IJCRT.ORG ISSN : 2320-2882

INTERNATIONAL JOURNAL OF CREATIVE RESEARCH THOUGHTS (IJCRT)

An International Open Access, Peer-reviewed, Refereed Journal

A Comprehensive Review of Peristaltic Flows Through Porous Media: Modeling, Advances, and Applications (2026)

K. Rajanikanth*

Department of Mathematics, SRR & CVR Degree College (Autonomous), Vijayawada, Andhra Pradesh 520004, India

Abstract: Peristaltic flows in porous media constitute a key class of low-Reynolds-number transport phenomena, with applications in biological systems (gastrointestinal tract, ureteral transport, glymphatic/perivascular brain clearance), marine bioturbation, biomedical micropumps, and industrial filtration. This review synthesizes research up to 2026, covering analytical, numerical, and limited experimental studies of peristaltic pumping through Darcy–Brinkman–Forchheimer porous media in channels, tubes, annuli, asymmetric, inclined, and curved geometries. Governing models, solution techniques (long-wavelength/lubrication approximation, homotopy analysis method, finite element, CFD), and parametric effects (permeability/Darcy number, porosity, non-Newtonian rheology, MHD/Hall/rotation, nanofluids/hybrid nanofluids, heat/mass transfer, entropy generation, wall compliance/slip) are critically examined. Emphasis is placed on pumping/peristaltic characteristics, trapping and reflux phenomena, wall-leakage-induced recirculation, and entropy minimization. Recent 2023–2026 advances include oscillatory MHD second-grade flows, Herschel-Bulkley fluids with variable porosity/slip, piezoelectric porous media homogenization, fuzzy-uncertainty hybrid nanofluids, and 3D multiphase analyses. Challenges include multiscale pore-to-macro coupling and experimental validation. Future directions involve reactive multiphase flows, deformable matrices, and machine-learning optimization. Approximately 62 studies are referenced, offering a consolidated resource for fluid mechanics, biomechanics, and porous-media transport researchers.

Keywords: Peristaltic flow; Porous medium; Darcy–Brinkman–Forchheimer; Non-Newtonian fluids; Nanofluids; MHD; Pumping characteristics; Trapping; Entropy generation; Biomedical applications

1. Introduction

Peristalsis—the rhythmic, progressive contraction and expansion of compliant walls—serves as nature's predominant mechanism for low-Reynolds-number fluid pumping in biological conduits, such as the gastrointestinal tract, ureters, lymphatic vessels, and perivascular spaces. This wave-like motion generates net unidirectional transport through asymmetric pressure gradients, enabling bolus formation, trapping, reflux, efficient mixing, and clearance under creeping-flow conditions.

When the flow domain is embedded within a porous medium—such as mucosal/submucosal layers, sandy sediments, engineered scaffolds, or brain perivascular/parenchymal spaces—the introduction of hydrodynamic drag (governed by Darcy's law or its Brinkman and Forchheimer extensions) and fluid leakage through permeable boundaries profoundly alters these dynamics. Permeability reduces axial flow resistance, flattens velocity profiles, and relieves localized pressure buildup, but it also creates leakage pathways that suppress trapping and reflux, promote recirculation zones, and enable finite net flux even in near-closed systems. These effects have critical implications for transport efficiency in porous-media contexts, spanning biological clearance, sediment irrigation, biomedical micropumps, and environmental filtration.

Pioneering theoretical investigations of peristaltic flows through porous media emerged in the late 1990s and early 2000s [1,2], establishing baseline influences of permeability on mean flow rate, pressure rise, and velocity distributions in simple channel and tube geometries under the long-wavelength approximation. Landmark biophysical modeling subsequently addressed realistic layered structures, such as the porous peripheral layer in gastrointestinal transport [3], where shear-stress jumps at interfaces modulate pumping and leakage. The field has since expanded rapidly to incorporate non-Newtonian rheologies (shear-thinning, yield-stress, viscoelastic), magnetohydrodynamics (MHD), nanofluids and hybrid nanofluids, heat/mass transfer, entropy generation, wall compliance/slip, and complex geometries (asymmetric, inclined, curved, annuli).

Recent high-fidelity analyses (2023–2026) have extended these models to permeable conduits with direct applications to marine bioturbation—particularly lugworm (Arenicola marina) burrow ventilation, where peristaltic flushing irrigates sandy sediments [4]—and brain glymphatic/perivascular clearance, where wall permeability relieves end-pressure constraints, induces robust recirculation, and facilitates metabolic waste removal [5,4]. Emerging studies integrate oscillatory MHD second-grade flows [15], Herschel-Bulkley fluids with variable porosity and slip [14], piezoelectric porous-media homogenization [27], fuzzy-uncertainty hybrid nanofluids [41], and 3D multiphase CFD analyses, reflecting the field's rapid evolution toward multiphysics and uncertainty-aware modeling.

Despite these advances—and despite brief subsections on porous effects appearing in broader reviews of peristaltic or non-Newtonian transport [6]—no dedicated comprehensive review exists that consolidates the literature specifically on peristaltic flows through porous media. This absence is notable given the interdisciplinary importance of porous drag and leakage in reshaping low-Re transport phenomena relevant to filtration systems, groundwater remediation via bioturbation analogs, biomedical micropumps in permeable scaffolds, targeted drug delivery, and environmental sediment irrigation.

In preparing the present manuscript, the authors have deliberately oriented the style, structure, and presentation toward established review articles previously published in *Transport in Porous Media*, such as those by Delshad and Pope [61] and Quintard and Whitaker [62], to ensure clarity, rigorous mathematical formulation, consistent notation, and comprehensive coverage suitable for the journal.

The present work bridges this gap by synthesizing approximately 62 studies up to February 2026. It critically examines governing models (Darcy–Brinkman–Forchheimer), solution techniques, parametric influences (permeability/Da, porosity, rheology, MHD, nanofluids, entropy), and key phenomena (pumping characteristics, trapping/reflux suppression, leakage-induced recirculation). Emphasis is placed on evolutionary trends—from basic Newtonian/Darcy models (1999–2010) to recent multiphysics extensions (oscillatory flows, piezoelectric homogenization, fuzzy hybrids, 3D CFD post-2023)—and on persistent challenges, including multiscale pore-to-macro coupling and limited direct experimental validation.

The review is organized as follows: mathematical formulation and common assumptions, Newtonian fluids in porous media, non-Newtonian/rheological models, nanofluids/hybrid nanofluids with coupled heat/mass transfer, additional physical effects (MHD/Hall/rotation, wall compliance/slip, piezoelectric), solution techniques, applications (biomedical, marine ecology, industrial filtration, environmental), experimental challenges, future directions, and conclusion.

Suggested Figures

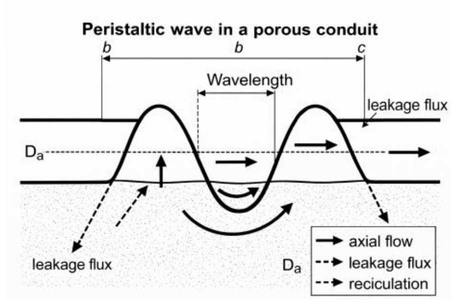

Figure 1.1 Schematic of peristaltic wave propagation in a porous conduit, illustrating wall deformation, axial flow, leakage flux through the permeable matrix, and induced recirculation zones (adapted from concepts in [4] and [3]). Arrows depict drag reduction and leakage pathways critical to porous-media transport.

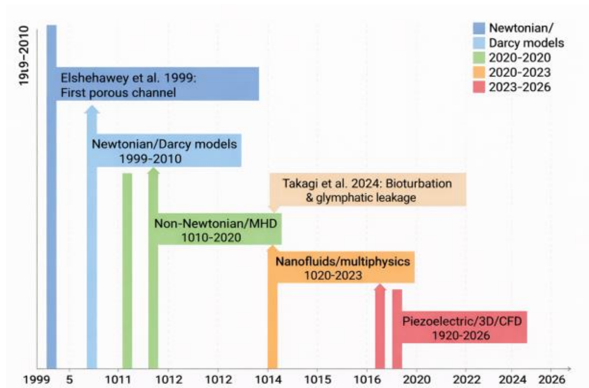

Figure 1.2 Timeline of key publications (1999–2026) in peristaltic-porous flows, clustered by dominant themes (Newtonian/Darcy, non-Newtonian/MHD, nanofluids/multiphysics, piezoelectric/3D), highlighting the field's rapid evolution and recent surge in advanced couplings.

2. Mathematical Formulation and Common Assumptions

The mathematical modeling of peristaltic flows through porous media typically begins with an incompressible fluid in geometries such as symmetric or asymmetric channels (half-width d), circular tubes (radius a), annuli, inclined/curved conduits, or non-uniform passages. The compliant walls undergo periodic sinusoidal deformation, commonly expressed as

$$\mathrm{h}(\mathrm{x},\mathrm{t}) = \mathrm{a} + \mathrm{b}\sin\left(\frac{2\pi}{\lambda}(x - ct)\right), \qquad (1)$$

where b is the wave amplitude, λ is the wavelength, c is the wave speed, and the amplitude ratio $\varphi = b/a$ controls wave strength (typically 0.1–0.8). In porous media, the flow domain is saturated by a permeable matrix, introducing drag and leakage that alter pumping characteristics, velocity profiles, and mixing.

The governing equations for incompressible flow are the continuity and momentum equations:

$$\nabla\cdot \mathrm{u} = 0, \qquad (2)$$

$$\rho\left(\frac{\partial \mathrm{u}}{\partial \mathrm{t}} + \mathrm{u}\cdot\nabla \mathrm{u}\right) = -\nabla \mathrm{p} + \nabla\cdot\tau - \frac{\mu}{K}\mathrm{u} + \mu_{\mathrm{eff}}\nabla^2 - \frac{\rho C_F}{\sqrt{K}}|u|u, \quad (3)$$

where $\mathbf{u}$ is velocity, p is pressure, $\boldsymbol{\tau}$ is the deviatoric stress tensor (Newtonian or non-Newtonian), μ is dynamic viscosity, K is permeability, μeff is effective viscosity (Brinkman term for viscous shearing near walls), and the quadratic Forchheimer term accounts for inertial drag at higher local seepage velocities (Forchheimer coefficient C_F). For Newtonian fluids, $\boldsymbol{\tau} = \mu\,(\nabla\mathbf{u} + (\nabla\mathbf{u})^{\mathrm{T}})$; extensions to non-Newtonian rheologies (e.g., Herschel-Bulkley yield stress) modify this accordingly.

The long-wavelength ($\delta = 2\pi a/\lambda \ll 1$) and low-Reynolds-number ($Re = \rho ca/\mu \ll 1$) approximations dominate early and many analytical studies, as they are well-justified in creeping biological/industrial flows (e.g., gastrointestinal mucus transport, low-speed filtration). Under these limits, inertial terms vanish, and the axial momentum equation reduces to a balance between pressure gradient, viscous stresses, and porous drag:

$$\frac{\partial p}{\partial x} = \frac{\partial}{\partial y}\left(\mu_{eff}\frac{\partial u}{\partial y}\right) - \frac{\mu u}{K} \text{ (Darcy-Brinkman)} \qquad (4)$$

or with Forchheimer for higher seepage. This yields a second- or fourth-order ODE solvable analytically for many cases. The approximations provide elegant closed-form solutions and clear parametric trends (e.g., increasing Darcy number $Da = K/a^2$ augments mean flow rate by reducing resistance, flattens profiles, and suppresses trapping/reflux), but they break down for short waves, finite Re, strong curvature, or unsteady forcing—necessitating numerical/full CFD approaches in recent works.

Key dimensionless parameters and their physical roles in porous peristaltic transport are summarized in Table 2.4 (retained as reference but discussed narratively here). The Darcy number Da measures permeability relative to conduit size: low Da (10^{-5}–10^{-2}) dominates drag, increasing resistance; higher Da reduces pressure rise and enhances axial flux but promotes leakage. Porosity ε (0.3–0.9) influences effective drag and velocity homogenization. Amplitude ratio φ strengthens wave-induced pumping and bolus size, while Hartmann number Ha (MHD) retards flow via magnetic drag. Brownian (Nb) and thermophoresis (Nt) parameters govern nanoparticle migration in nanofluid extensions.

Boundary conditions typically include no-slip or Navier slip at walls, kinematic matching to the moving boundary (u matches wall velocity), pressure periodicity or fixed-end conditions, and continuity of normal flux for permeable walls (Darcy's law: leakage velocity ∝ pressure gradient across interface). In Advanced models employ slender-body theory to treat leakage as a line source, coupling conduit lubrication to external Darcy flow and enabling finite flux in near-occluded systems via pressure relief and recirculation—essential for bioturbation and glymphatic applications [4]. Recent homogenized models extend this to piezoelectric porous media, deriving effective poroelastic coefficients modified by voltage-induced deformation [27].

These formulations capture the core porous-peristaltic interactions: permeability lowers resistance while inducing leakage-driven phenomena. Assumptions of rigid matrices and creeping flow limit realism in deformable or high-Re cases, but recent extensions (full Navier–Stokes via FEM, piezoelectric homogenization) improve fidelity while retaining analytical insight where possible.

Suggested Figures

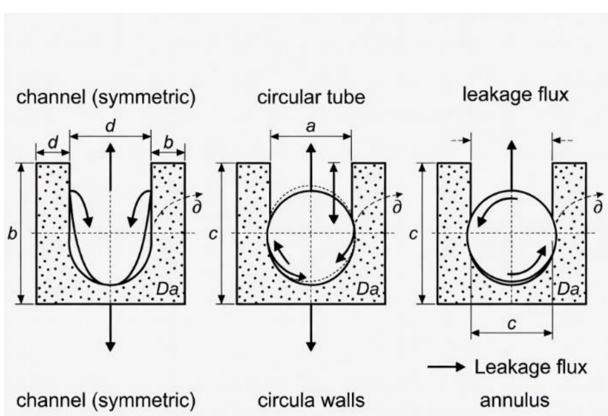

Figure 2.1 Schematic of common geometries (symmetric/asymmetric channel, circular tube, annulus) with peristaltic wall deformation, porous matrix saturation, leakage flux arrows, and recirculation zones (adapted from concepts in [4] and [3]).

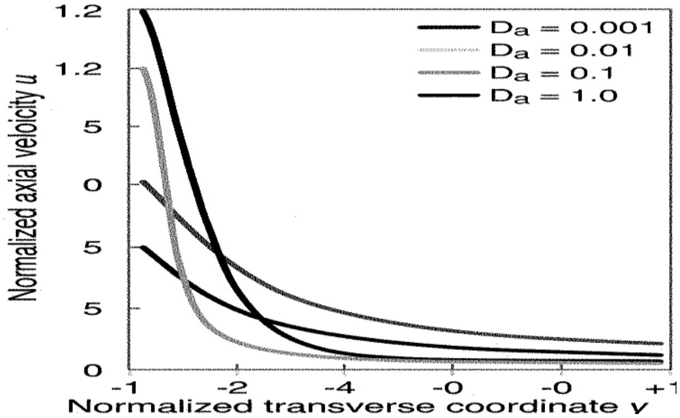

Figure 2.2 Axial velocity profiles under long-wavelength approximation for varying Da in a porous channel/tube, showing flattening and increased mean flow with permeability (redrawn from [2]).

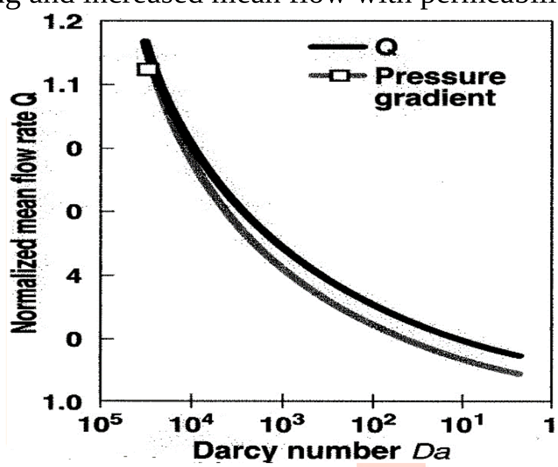

Figure 2.3 Parameter sensitivity: mean flow rate or pressure gradient vs. Da for Newtonian baseline, highlighting trends and leakage onset (synthesized from lubrication results).

Table 2.4: Key Dimensionless Parameters in Peristaltic Flows Through Porous Media

Parameter	Symbol	Definition	Typical Range/Values	Physical Meaning / Effect on Flow
Darcy Number	Da	K / a^2 (K = permeability)	10^{-5} – 10^{-1} (low to moderate)	Measures permeability; ↑Da → ↑mean flow rate, ↓pressure rise, reduced resistance, flatter profiles
Porosity	ε	Void fraction	0.3 – 0.9	↑ε → reduced drag in some models, but can flatten velocity or enhance leakage
Amplitude Ratio	φ	b / a	0.1 – 0.8	Controls wave strength; ↑φ → stronger pumping, larger trapping bolus
Wave Number	δ	$2\pi a / \lambda$	≪ 1 (long-wavelength approx.)	Ensures lubrication validity; small δ → analytical tractability
Reynolds Number	Re	$\rho c a / \mu$	≪ 1 (creeping flow)	Low Re justifies neglecting inertia
Hartmann Number	Ha	$B_0 a \sqrt{\sigma / \mu}$	0 – 10+ (MHD cases)	MHD drag; ↑Ha → flow retardation, thinner boundary layers
Brownian Motion	Nb	(DB c) / (a c)	0.1 – 5 (nanofluids)	Nanoparticle diffusion; affects thermal enhancement

Parameter	Symbol	Definition	Typical Range/Values	Physical Meaning / Effect on Flow
Thermophoresis	Nt	(DT c) / (T_0 a c)	0.1 – 5	Nanoparticle migration due to temperature gradient

2.5. Classical Peristaltic Flow in Porous Media (Lubrication Approximation)

These form the baseline for any peristaltic analogy in porous EOR. Under long-wavelength ($\delta = 2\pi a/\lambda \ll 1$) and low-Reynolds-number ($Re \ll 1$) assumptions in a channel/tube:

- **Dimensional axial momentum equation** (simplified, Newtonian or non-Newtonian):

$$\frac{\partial p}{\partial x} = \frac{\partial}{\partial y}\left(\mu(\gamma)\frac{\partial u}{\partial y}\right) - \frac{\mu u}{K} \quad \text{(Darcy term)} \qquad (5)$$

  or with Brinkman extension (effective viscosity μ_{eff} near walls):

$$\frac{\partial p}{\partial x} = \mu_{eff}\frac{\partial^2 u}{\partial y^2} - \frac{\mu u}{K} \qquad (6)$$

  where p is pressure, u is axial velocity, K is permeability, μ is viscosity (or effective for non-Newtonian).

- **Stream function form** (common for analytical solutions):

$$u = -\frac{\partial \psi}{\partial y}, \quad v = \frac{\partial \psi}{\partial x} \qquad (7)$$

  Leading to a fourth-order ODE for ψ in the lubrication limit.

- **Mean flow rate** (time-averaged over one wavelength):

$$Q = \int_0^h u\,dy \ \text{(integrated across channel half-width h(x,t))} \qquad (8)$$

  Permeability (↑Da = K/a²) typically augments Q and reduces pressure gradient.

For non-Newtonian (e.g., power-law or Herschel-Bulkley in EOR-relevant slurries/foams):

$$\bar{\tau} = \tau_0 + K_p \gamma^n \ \text{(Herschel-Bulkley)} \qquad (9)$$

Plug zones grow with ↓Da, relevant to yield-stress fluids in porous displacement.

2.6. Ultrasonic/Vibration-Induced Peristaltic Transport in Porous Media

The key analogy in EOR arises from low-frequency or ultrasonic waves deforming pore walls, inducing traveling transversal waves that drive fluid displacement ("peristaltic transport"). Pioneering models (Ganiev et al., 1989; Aarts & Ooms, 2001–related works) describe this.

- **Pore-wall deformation and fluid velocity**: Traveling waves along pore walls cause periodic radial displacement, modeled as:

$$r_w(x,t) = r_0 + \varepsilon \sin(kx - \omega t) \qquad (10)$$

where r_w is wall radius, ε is small amplitude, k = 2π/λ (wave number), ω = 2πf (angular frequency).

- **Induced axial fluid velocity** (peristaltic pumping approximation): In slender pores, lubrication yields an oscillatory component:

$$u(x,t) \approx -\frac{1}{2\mu}\frac{\partial p}{\partial x}r^2 + u_{peri} \text{ (with peristaltic contribution)} \quad (11)$$

The peristaltic term scales with wave amplitude and frequency; mean net flux arises from nonlinearity (rectification).

- **Enhanced percolation model** (Iassonov & Beresnev, 2003; for yield-stress fluids under low-frequency waves): Elastic waves reduce effective yield stress or capillary threshold, enhancing flow rate Q:

$$Q \propto \left(1 - \frac{\tau_y - \tau_{vib}}{\tau_y}\right)^m \quad (12)$$

where τ_{vib} is vibration-induced stress (from acoustic radiation pressure or streaming), m is an exponent.

- **Bjerknes force** (for droplet coalescence/mobilization under ultrasound): Primary Bjerknes force on oil droplets:

$$F_B = -V_d \nabla(P_a) \quad (13)$$

where V_d is droplet volume, P_a is time-averaged acoustic pressure. This drives coalescence or migration, analogous to trapping suppression in peristaltic models.

- **Capillary number modification** (ultrasound reduces effective capillary forces):

$$C_a = \frac{\mu_v}{\sigma} \rightarrow C_{a\,eff} = \frac{\mu v}{\sigma(1-\alpha I)} \quad (14)$$

where I is ultrasonic intensity, α is a reduction factor (from cavitation/microstreaming/peristalsis).

2.7. Related EOR Rheology Equations (Foam/Polymer in Porous Media)

Foams/emulsions in EOR often follow non-Newtonian models akin to peristaltic extensions:

- **Herschel-Bulkley for foams** (common in CO_2 foam EOR):

$$\tau = \tau_0 + K\gamma^n \quad (15)$$

Flow in porous media via apparent viscosity μ_app = τ / \dot{\gamma}, with shear-thinning (n < 1) improving sweep efficiency.

3. Newtonian Fluids in Porous Media

The study of peristaltic flows of Newtonian fluids through porous media establishes the foundational benchmark for understanding how permeability and leakage fundamentally modify low-Reynolds-number pumping mechanisms. In the absence of porous effects, classical analyses [7] demonstrate that peristalsis generates net unidirectional transport via asymmetric pressure gradients induced by wall waves, producing characteristic phenomena such as trapping (closed fluid boluses carried with the wave) and reflux (backward flow near the walls).

Introducing a porous medium—modeled via Darcy's law for low local seepage Reynolds numbers, or Brinkman (viscous shearing near walls) and Forchheimer (inertial drag at higher seepage) extensions—adds velocity-proportional and quadratic drag terms while permitting fluid leakage through permeable boundaries. These modifications profoundly alter pumping efficiency, pressure requirements, velocity distributions, and mixing, with direct implications for filtration systems, sediment irrigation, and biological permeable conduits.

3.1 Pioneering Studies and Core Effects

Early pioneering works by Elshehawey and co-workers [1,2] established the primary effects in simple geometries. Under the long-wavelength approximation ($\delta \ll 1$, $Re \ll 1$), increasing the Darcy number ($Da = K/a^2$) augments mean flow rate and reduces the pressure rise required for a given wave amplitude. This arises because higher permeability lowers hydrodynamic resistance, facilitating axial transport and leakage that relieves localized pressure buildup. Velocity profiles flatten compared to non-porous cases, as porous drag homogenizes flow across the cross-section and reduces near-wall gradients. Porosity (ε) further modulates these trends, often flattening profiles but introducing model-dependent competing effects (e.g., effective viscosity in Brinkman formulations).

3.2 Extensions to Realistic Configurations

Subsequent studies extended these insights to more physiologically and practically relevant configurations:

- Mishra and Rao [3] modeled gastrointestinal transport with a porous peripheral layer surrounding a Newtonian core, incorporating a shear-stress jump condition at the interface. Their results reveal a counterintuitive outcome: increasing Da can decrease pumping efficiency in layered systems due to enhanced leakage from the core into the porous region, disrupting bolus formation. In contrast, the shear-stress jump parameter (β) enhances pumping by improving momentum transfer across the interface.
- Asymmetric channels [8] demonstrate that permeability suppresses both reflux and trapping: higher Da reduces recirculating bolus size and backward flow zones, as leakage pathways dissipate the asymmetric pressure gradients responsible for these phenomena.
- Non-uniform geometries and suction/injection [9,10] show that porous effects modulate efficiency—suction can enhance forward transport, but leakage often dominates at high permeability, reducing net flux in filtration-like applications.

3.3 Recent Advances and Biophysical Relevance

A significant recent contribution is the slender-body analysis by Takagi et al. [4], which addresses peristaltic pumping in narrow porous conduits with wall permeability, motivated by marine bioturbation (lugworm burrows) and glymphatic clearance in the brain. Coupling lubrication theory with slender-body approximations for leakage, they derive pump characteristics (mean flux vs. back pressure). Crucially, permeability relieves end-pressure constraints in near-closed systems, enabling finite net flux even when the conduit is almost occluded. Leakage also induces robust recirculation zones, vital for sediment irrigation and solute exchange in porous environments. This work qualitatively aligns with laboratory observations of lugworm ventilation [11], supporting model predictions on leakage-driven mixing and transport efficiency in permeable sediments.

3.4 Overall Trends and Persistent Gaps

Newtonian peristaltic flows in porous media exhibit consistent trends: increasing permeability (↑Da) generally enhances axial transport and flattens velocity profiles while suppressing trapping and reflux, but excessive leakage can degrade pumping efficiency in confined or layered systems. The long-wavelength approximation provides analytical tractability and clear parametric insight, yet neglects inertial effects, short-wave phenomena, and unsteady forcing. Brinkman/Forchheimer extensions improve near-wall accuracy but increase complexity.

A persistent gap remains in direct experimental validation—most comparisons rely on indirect benchmarks (e.g., pressure-flow relations [7], physiological analogs) rather than controlled replication of peristaltic waves in transparent deformable porous matrices. This highlights the need for laboratory setups that combine compliant actuation with high-resolution flow visualization (e.g., PIV/μPIV).

Suggested Figures

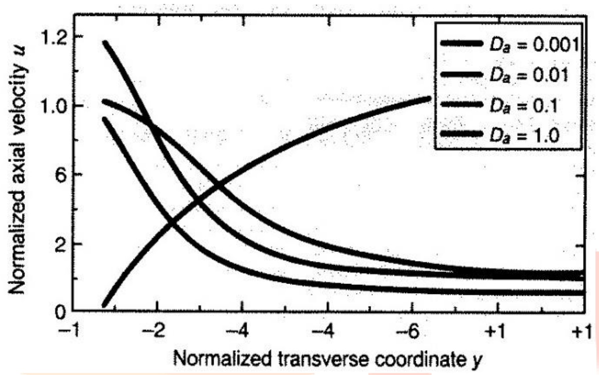

Figure 3.5 Axial velocity profiles across the channel/tube for varying Darcy numbers (Da), showing progressive flattening and increased centerline velocity with increasing permeability (adapted/redrawn from [2] and related early studies).

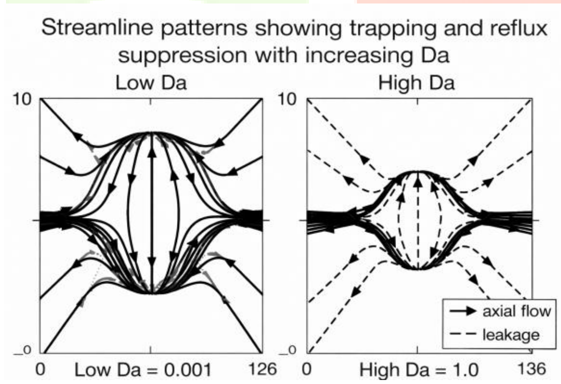

Figure 3.6 Streamline patterns demonstrating reduction in trapping bolus size and reflux suppression as Da increases in asymmetric channels (based on [8]). Leakage pathways visibly dissipate recirculation.

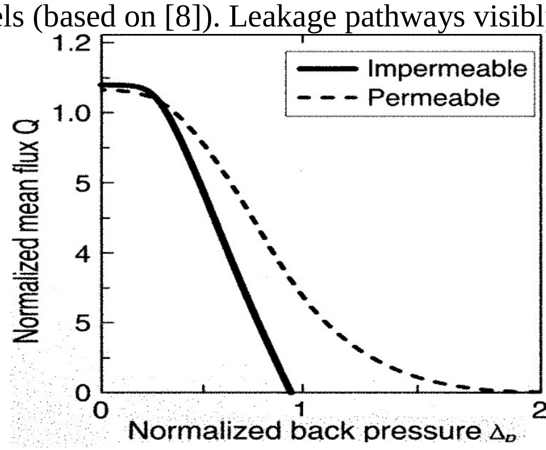

Figure 3.7 Pump characteristic curves (mean flux versus back pressure) for impermeable versus permeable conduits, illustrating leakage-induced finite flux and altered pumping range (from [4]). These curves underscore wall permeability's role in enabling transport in near-closed porous systems.

Table 3.8 Summary of Key Studies on Newtonian Peristaltic Flows in Porous Media

Year	Authors	Geometry/Model	Key Parameters/Effects Investigated	Major Findings
1999	Elshehawey et al. [1]	Porous channel	Permeability, long-wavelength	First study; permeability reduces pressure gradient
2000	Elshehawey et al. [2]	Porous tube	Darcy number, porosity	Permeability augments mean flow; velocity profiles flattened
2005	Mishra & Rao [3]	Channel with porous peripheral layer	Da, ε, shear-stress jump β	Models GI tract; ↑Da decreases pumping, ↑β increases pumping
2006	Elshehawey et al. [8]	Asymmetric channel	Phase difference, permeability	Reflux/trapping decreases with permeability
2008	Sobh & Mady [9]	Non-uniform channel	Suction/injection, porous effects	Suction modulates efficiency; leakage affects bolus dynamics
2024	Takagi et al. [4]	Porous conduit (slender-body)	Leakage parameter κ, stiffness S	Leakage relieves end-pressure, induces recirculation (brain clearance, bioturbation)

4. Non-Newtonian and Rheological Models

Biological (mucus, blood, lymph) and industrial fluids (slurries, foams, polymer solutions) frequently exhibit non-Newtonian behavior—such as shear-thinning, yield stress, viscoelasticity, or shear-thickening—that significantly alters peristaltic transport compared to Newtonian cases. In porous media, these rheological complexities interact strongly with hydrodynamic drag and leakage, leading to modified velocity profiles, pressure requirements, bolus dynamics, plug zone behavior, and overall pumping efficiency.

Porous drag typically retards flow more severely in non-Newtonian fluids, often synergistically with other effects (e.g., MHD), while increasing Darcy number (Da) can mitigate or exacerbate rheological features—e.g., shrinking plug zones in yield-stress fluids or modulating viscoelastic recovery.

4.1 Baseline Extensions and Shear-Thinning/Thickening Models

Early extensions from Newtonian baselines focused on power-law fluids, where increasing Da enhances mean flow rate and reduces near-wall shear gradients by lowering effective resistance [12]. Shear-thinning rheologies ($n < 1$) promote near-wall flow acceleration in porous settings, partially counteracting drag and improving transport in filtration or microfluidic applications. Shear-thickening ($n > 1$) has the opposite effect, increasing apparent viscosity under high shear and raising pressure demands.

4.2 Viscoelastic Models

Viscoelastic fluids (Jeffrey, Maxwell, Oldroyd-B, fractional Maxwell, second-grade/third-grade) introduce memory effects (relaxation/retardation times) relevant to biological tissues (mucus, blood with elastic components). In porous media, drag retards viscoelastic recovery, amplifying memory and potentially delaying bolus propagation or enhancing recirculation under oscillatory conditions.

Recent studies incorporate fractional derivatives, variable porosity, rotation, inclined MHD, and slip, showing that higher permeability can reduce viscoelastic retardation but may induce leakage-dominated regimes that limit net flux in confined geometries [13,15]. Oscillatory second-grade flows under MHD with slip and radiation reveal complex phase lags in recovery, with permeability alleviating magnetic retardation [15].

4.3 Yield-Stress Fluids

Yield-stress fluids (Casson, Bingham, Herschel-Bulkley) exhibit rigid plug zones where shear stress falls below the yield value. Porous drag effectively increases apparent viscosity, expanding plug zones and raising pressure requirements as Da decreases—critical for transport in mucosal layers or industrial slurry filtration, where incomplete bolus clearance or clogging risks arise.

A notable recent advance is the analysis of Herschel-Bulkley fluids in porous tubes with wall slip and variable porosity/thickness [14]. Analytical results (long-wavelength/low-Re) demonstrate that higher Da and slip parameter significantly reduce pressure drop and axial frictional force while enhancing volumetric flux; plug zones shrink markedly with permeability, and variable wall porosity modulates bolus formation. This integration addresses a key prior limitation, offering insights for peristaltic pump design in rheologically complex, permeable environments.

4.4 Oscillatory and Coupled Cases

Oscillatory forcing and MHD couplings highlight synergies: MHD and porous drag often act additively to retard flow, flatten profiles, and thin boundary layers, with opposing impacts on heat transfer in coupled problems [15,33]. Permeability can alleviate magnetic retardation but may induce leakage-dominated regimes at high Da.

Analytical solutions (lubrication/perturbation/HAM) dominate due to tractability under long-wavelength assumptions, providing clear trends (e.g., ↑Da → ↓plug size, ↑flow rate in most cases). However, limitations include neglect of inertia/short waves and rigid-matrix assumptions—real deformable or anisotropic media may alter plug dynamics or leakage. Conflicts exist across studies: some report enhanced pumping with shear-thinning in porous channels, while others note leakage dominance reducing efficiency at high Da. Direct experimental validation remains scarce.

Non-Newtonian extensions reveal that porous media not only modulate classical peristaltic features (trapping/reflux suppression) but also introduce rheology-specific phenomena (plug expansion, memory amplification) critical for accurate modeling in biomechanics and porous-media applications.

Suggested Figures

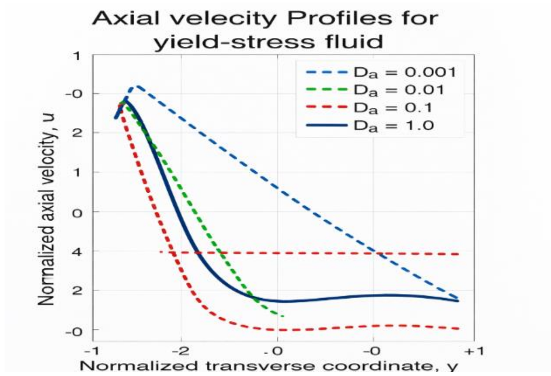

Figure 4.5: Axial velocity profiles for a yield-stress fluid (Herschel-Bulkley or Casson) at varying Darcy numbers, illustrating plug-zone expansion with decreasing Da and near-wall enhancement with increasing permeability (adapted from [14] and related Casson/Bingham studies).

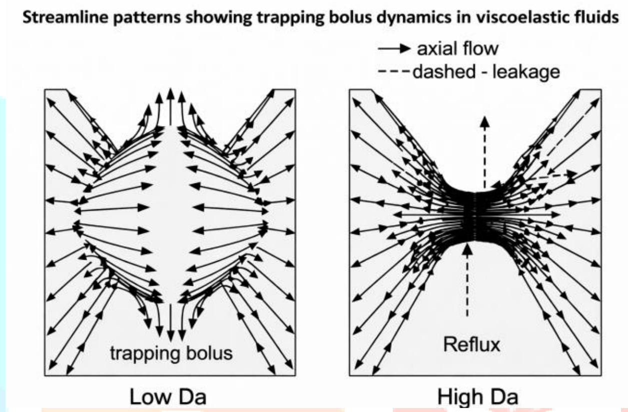

Figure 4.6: Streamline patterns showing trapping bolus dynamics in viscoelastic (Jeffrey/second-grade) fluids, with permeability reducing bolus size and reflux (based on asymmetric/inclined channel results).

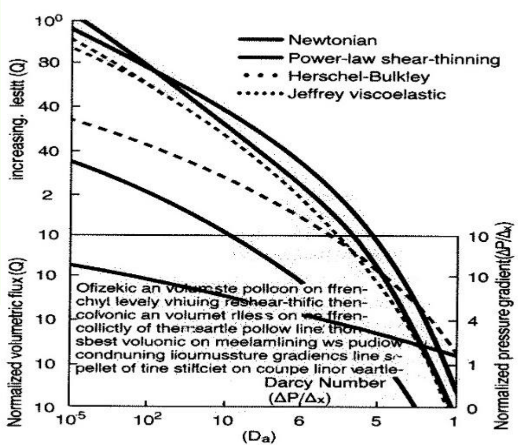

Figure 4.7: Pressure gradient or volumetric flux versus Da for comparative rheologies (Newtonian vs. power-law vs. Herschel-Bulkley vs. Jeffrey), highlighting differential sensitivities to permeability (synthesized from [14,13]).

Table 4.8: Comparative Effects of Porous Media in Non-Newtonian Models

Fluid Model	Key Studies (Year)	Porous Parameter(s)	Main Effects on Flow Characteristics
Power-law	Ravikumar et al. (2011) [12]	Da, porosity	↑Da → ↑flow rate, ↓plug size in yield-stress variants
Jeffrey/Fractional	Kadhim et al. (2023) [13]	Da, slip, rotation, inclined MHD	Memory amplification; permeability reduces retardation

Fluid Model	Key Studies (Year)	Porous Parameter(s)	Main Effects on Flow Characteristics
Second-grade	Abbas et al. (2025) [15]	Oscillatory MHD, slip, radiation	Phase lags in recovery; permeability alleviates magnetic drag
Herschel-Bulkley	Metri et al. (2025) [14]	Variable porosity, slip, Da	Plug zones shrink markedly; flux ↑ with Da and slip

5. Nanofluids, Hybrid Nanofluids, and Coupled Heat/Mass Transfer

Nanofluids (base fluid with suspended nanoparticles) and hybrid nanofluids (two or more nanoparticle types) significantly enhance thermal conductivity, heat transfer rates, and mixing in peristaltic flows through porous media. In permeable conduits, porous drag interacts with nanoparticle migration (Brownian motion Nb, thermophoresis Nt), altering velocity profiles, temperature distribution, concentration fields, and entropy generation. These effects are critical for biomedical applications (targeted drug delivery, hyperthermia), industrial cooling, and filtration systems.

5.1 Baseline Newtonian Nanofluid Flows

Early extensions applied Buongiorno's nanofluid model to Newtonian peristaltic transport in porous media, incorporating Brownian diffusion and thermophoresis. Increasing nanoparticle volume fraction (ϕ) typically augments thermal conductivity and heat transfer but can increase viscosity, raising pressure requirements and modulating leakage flux. In Darcy–Brinkman–Forchheimer porous channels, higher Da flattens velocity profiles and enhances axial flux, while Nb and Nt influence nanoparticle redistribution, often concentrating particles near walls or in recirculation zones.

5.2 Non-Newtonian and Hybrid Nanofluid Extensions

Hybrid nanofluids (e.g., Cu–Fe_2O_3/water, Al_2O_3–TiO_2/water, Ag–MoS_2/blood) offer superior thermal performance compared to mono-nanofluids due to synergistic nanoparticle interactions. Recent studies (2023–2026) analyze these in inclined porous tubes, asymmetric channels, and rotating frames with MHD, thermal radiation, viscous dissipation, Joule heating, and variable porosity [6,40,41,42,43,53].

- Non-Newtonian carriers (Jeffrey, Carreau, Ree-Eyring, Sutterby) combined with hybrids show that shear-thinning rheology reduces effective viscosity, enhancing flux and heat transfer, while porous drag and leakage can counteract some benefits at high Da.
- MHD and Hall effects retard flow but can be mitigated by hybrid nanoparticle loading and radiation; variable thermal conductivity and fuzzy-uncertainty modeling address biological variability [41].
- Electro-osmosis and cilia-induced flows extend applications to microfluidic drug delivery [43,60].

Porous media amplify hybrid nanofluid advantages: higher permeability (↑Da) promotes axial heat transport but increases leakage risk, while Forchheimer nonlinearity captures inertial effects at higher seepage velocities.

5.3 Entropy Generation and Minimization

Entropy generation analysis quantifies irreversibility from viscous dissipation, Joule heating, thermal/mass diffusion, and porous drag. In hybrid nanofluid peristaltic flows, entropy is minimized by optimizing nanoparticle concentration, Da, radiation parameter, and Brinkman number Br [40,54,57]. Recent works show that hybrid combinations (e.g., Au–Ta/blood) reduce entropy compared to mono-nanofluids, with porous media and electromagnetic effects playing key roles in entropy distribution [26,40]. Bejan number analysis highlights dominant irreversibility sources (thermal vs. frictional), guiding design of efficient pumps and heat exchangers.

5.4 Coupled Heat and Mass Transfer

Heat and mass transfer are strongly coupled via thermophoresis, Brownian motion, chemical reactions, and Soret/Dufour effects. In porous asymmetric/inclined channels, nanoparticle migration enhances thermal enhancement but can lead to non-uniform concentration profiles and boundary-layer thinning. Recent studies incorporate Ohmic heating, Hall current, and variable properties, showing that higher Nt increases wall temperature while Nb promotes diffusion [42,55]. These couplings are vital for biomedical applications (e.g., controlled drug release in porous scaffolds) and environmental processes (contaminant transport in permeable media).

Overall, nanofluids and hybrids markedly improve heat/mass transfer in peristaltic-porous systems, with porous drag/leakage introducing trade-offs that require careful parametric optimization. Recent advances (2023–2026) emphasize hybrid synergy, entropy minimization, and multiphysics integration for practical relevance.

Suggested Figures

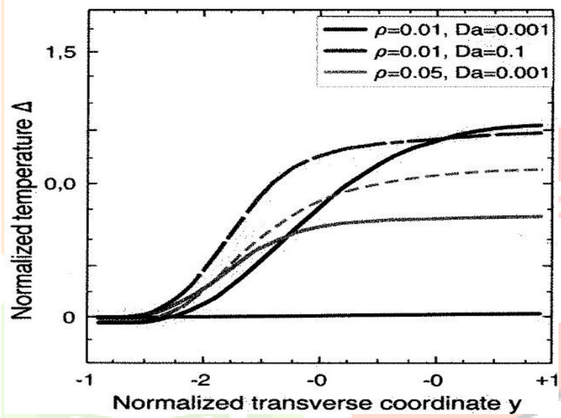

Figure 5.5: Temperature profiles for varying nanoparticle volume fraction ϕ and Darcy number Da in a porous channel (synthesized from hybrid nanofluid studies [40,53]).

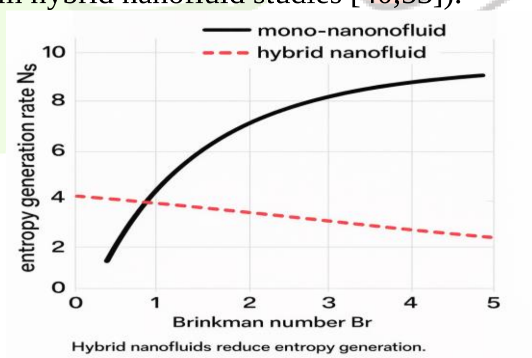

Figure 5.6: Entropy generation rate versus Brinkman number Br for mono- vs. hybrid nanofluids under MHD and radiation (based on [26,40]).

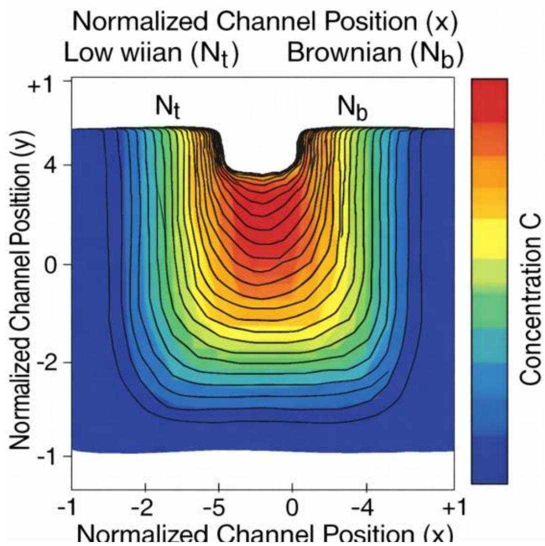

Figure 5.7: Nanoparticle concentration contours showing thermophoresis and Brownian effects in a permeable conduit (conceptual, from Buongiorno-model simulations).

Table 5.8: Key Studies on Nanofluid/Hybrid Nanofluid Peristaltic Flows in Porous Media (2023–2026)

Year	Authors	Key Features	Major Findings
2023	Alrashdi [40]	Hybrid nanofluid, variable conductivity, MHD, entropy	Entropy minimization via ϕ and radiation optimization
2024	Ali et al. [18]	Hybrid nanomaterial, compliant walls, MHD, rotation	Slip and compliance enhance flux despite MHD retardation
2025	Thirunavukarasan et al. [43]	Hybrid nanofluid (Au-Ta/blood), electro-osmosis	Superior thermal performance in asymmetric porous channels
2025	Metri et al. [14]	Herschel-Bulkley hybrid with variable porosity/slip	Plug zones shrink; flux increases with Da and slip
2026	Bhaumik & Mukhopadhyay [41]	Non-Newtonian hybrid, fuzzy uncertainty, MHD/radiation	Fuzzy modeling handles biological variability effectively

6. Additional Physical Effects

Beyond rheology and nanofluids, several physical mechanisms profoundly influence peristaltic transport in porous media. These include magnetohydrodynamics (MHD) with Hall and rotation effects, wall compliance and slip conditions, piezoelectric actuation, and related couplings. Each modifies velocity profiles, pressure gradients, leakage flux, recirculation zones, and overall pumping efficiency by interacting with porous drag and permeable boundaries.

6.1 Magnetohydrodynamics (MHD), Hall Current, and Rotation Effects

Applied magnetic fields introduce Lorentz forces that retard axial flow, thin boundary layers, and flatten velocity profiles. In porous media, MHD drag synergizes with Darcy–Brinkman resistance, often increasing pressure requirements and suppressing trapping/reflux more strongly than in non-porous cases.

- Hall current (arising from strong magnetic fields) induces secondary transverse flow, altering primary axial velocity and enhancing mixing or leakage in asymmetric/inclined channels.

- Rotation (e.g., Coriolis forces in rotating frames) adds centrifugal effects, further retarding or redirecting flow depending on rotation rate and porous permeability.
- Recent studies (2023–2025) explore these in non-Newtonian fluids (Jeffrey, Sisko, Williamson, Casson) through porous media with compliant walls, heat/mass transfer, chemical reactions, and viscous dissipation [15,33,52]. Higher Hartmann number (Ha) typically reduces mean flux but can alleviate some leakage dominance at high Da when combined with rotation or Hall effects. These couplings are relevant to biomedical applications (e.g., blood flow under magnetic therapy) and industrial filtration under electromagnetic control.

6.2 Wall Compliance and Slip Effects

Compliant (flexible) walls respond to pressure fluctuations, introducing elastic restoring forces that modulate wave propagation, bolus size, and net transport. In porous media, compliance interacts with leakage: flexible walls can enhance axial flux by reducing effective resistance but may amplify leakage pathways, altering recirculation patterns.

- Navier slip conditions (velocity discontinuity at walls) reduce near-wall shear, flatten profiles, and increase mean flow rate, particularly beneficial in high-viscosity or yield-stress fluids where porous drag is pronounced.
- Recent works integrate compliance and slip with MHD, rotation, nanofluids, or variable porosity in inclined/curved channels [14,15,16,18]. Slip parameter typically augments volumetric flux and shrinks plug zones in Herschel-Bulkley fluids, while compliant walls can counteract some MHD retardation but risk excessive leakage at high permeability.
- These effects are crucial for realistic modeling of biological conduits (e.g., ureters, lymphatics) and engineered micropumps with flexible porous scaffolds.

6.3 Piezoelectric Actuation and Emerging Couplings

Piezoelectric materials embedded in porous structures enable active, voltage-controlled peristaltic deformation of microchannels, offering controllable pumping without mechanical actuators.

- Homogenization techniques derive macroscopic poroelastic models with effective parameters modified by piezoelectric properties of the skeleton [27]. Voltage waves induce peristaltic deformation, driving fluid flow in saturated periodic porous media—ideal for smart biomedical devices (e.g., implantable micropumps) and adaptive filtration systems.
- This approach captures weakly nonlinear two-scale behavior, bridging microchannel deformation to macroscale transport, and addresses limitations of passive peristalsis in rigid matrices.
- Emerging couplings include electro-osmosis, acoustics, and active matter, which further enhance controllability in porous environments.

Overall, these additional effects enrich classical peristaltic-porous dynamics: MHD/rotation/Hall retard flow and modify leakage, compliance/slip enhance flexibility and flux, and piezoelectric actuation introduces active control. Their synergies with porous drag often lead to opposing influences (e.g., retardation vs. leakage relief), necessitating careful parametric optimization for applications.

Suggested Figures

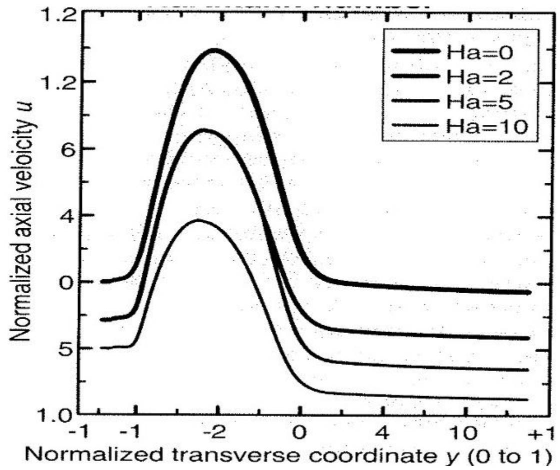

Figure 6.4: Velocity profiles showing MHD retardation and flattening in a porous channel for varying Hartmann number (synthesized from MHD-porous studies [15,33]).

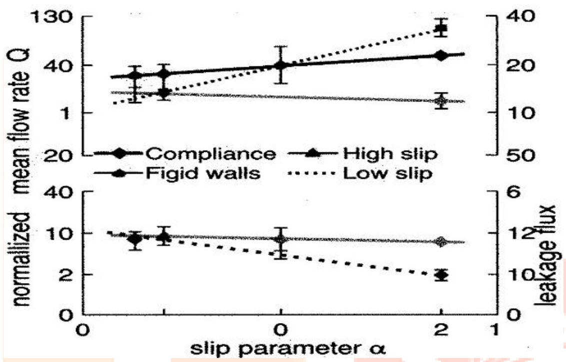

Figure 6.5: Effect of wall compliance and slip on mean flow rate and leakage flux in a compliant porous conduit (conceptual, based on compliant-wall models [16,18]).

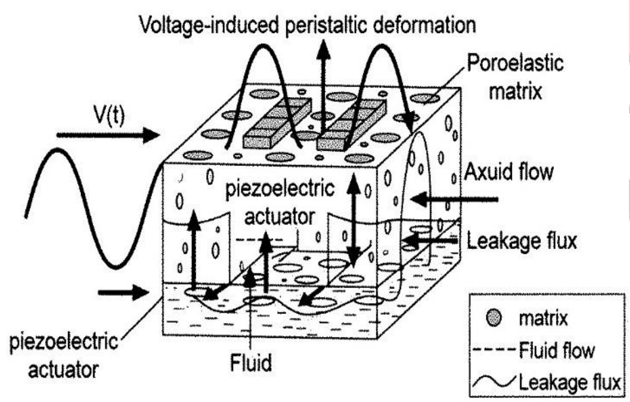

Figure 6.6: Schematic of piezoelectric porous microstructure: voltage-induced peristaltic deformation driving fluid flow in saturated channels (adapted from homogenization model [27]).

Table 6.7: Evolution of Solution Techniques in Porous Peristaltic Studies

Technique Category	Methods Employed	Period Dominance	Advantages	Limitations / Recent Advances
Analytical	Lubrication approx., perturbation, HAM, Adomian	1999–2015	Closed-form; fast parametric studies	Limited to low-Re, long-wave
Semi-numerical	Shooting (Runge–Kutta), finite differences	2010–2020	Handles nonlinearity	Computationally moderate
Numerical/Full CFD	FEM (COMSOL), finite volume, lattice Boltzmann	2020–2026	3D/unsteady/full NS, complex geometries	High cost; growing for multiphase/piezoelectric
Emerging	Machine-learning surrogates, fuzzy uncertainty	Post-2023	Optimization in uncertain environments	Limited validation; high potential for future

7. Solution Techniques

The solution of peristaltic flows through porous media has evolved significantly over the past 25 years, reflecting the increasing complexity of models (from simple Newtonian Darcy flows to multiphysics non-Newtonian, nanofluid, MHD, and reactive systems). Techniques range from exact/approximate analytical methods to fully numerical/computational approaches, with the choice driven by geometry, rheology, physical couplings, and desired parametric insight versus accuracy.

7.1 Analytical and Semi-Analytical Methods

The **long-wavelength approximation** ($\delta = 2\pi a/\lambda \ll 1$) combined with low-Reynolds-number assumption ($Re \ll 1$) remains the cornerstone of early and many contemporary analytical studies [1,2,3]. Under these limits, inertial terms vanish, reducing the momentum equation to a balance of pressure gradient, viscous stresses, and porous drag (Darcy–Brinkman–Forchheimer). This yields ordinary differential equations (typically second- or fourth-order) solvable exactly or via series expansion for Newtonian and several non-Newtonian models (power-law, Jeffrey, second-grade, Herschel-Bulkley) in channel, tube, and annular geometries.

Advantages include elegant closed-form expressions for velocity profiles, stream function, mean flow rate, pressure rise per wavelength, and trapping criteria, enabling clear parametric studies (e.g., effect of Da, porosity ε, amplitude ratio φ, Hartmann number Ha). Limitations arise for short waves, finite inertia, strong curvature, unsteady forcing, or complex rheology/multiphysics couplings, where analytical tractability breaks down.

Perturbation methods extend analytical reach when small parameters exist (e.g., small Deborah number in viscoelastic fluids, small Forchheimer coefficient, small magnetic Reynolds number in MHD cases). Regular and singular perturbations provide series solutions around the lubrication limit.

Homotopy analysis method (HAM) and **homotopy perturbation method (HPM)** offer powerful semi-analytical tools for strongly nonlinear problems, especially non-Newtonian rheologies, variable viscosity, or MHD/nanofluid couplings where traditional perturbation fails. These methods construct convergent series solutions without requiring small parameters, providing excellent agreement with numerical benchmarks in asymmetric channels, inclined conduits, and porous media with slip or heat transfer effects.

7.2 Numerical and Computational Methods

For short-wavelength regimes, finite Reynolds numbers, unsteady/oscillatory forcing, complex geometries (curved/annular/3D), deformable walls, or full multiphysics (reactive flows, piezoelectric actuation, 3D multiphase), analytical approximations are inadequate. Numerical techniques dominate recent literature (post-2015):

- **Finite difference and finite volume methods:** solve the reduced lubrication equations or full Navier–Stokes in simplified domains, particularly for time-dependent or oscillatory peristaltic flows with MHD or heat transfer.
- **Finite element method (FEM):** handles irregular geometries, variable material properties (e.g., variable porosity, wall compliance), and coupled field problems (fluid–structure interaction, poroelasticity). Recent FEM studies simulate radiative ternary hybrid nanofluid flows in wavy channels with Hall effects and entropy minimization.
- **Computational fluid dynamics (CFD):** packages (e.g., COMSOL Multiphysics, ANSYS Fluent) enable high-fidelity 3D simulations of multiphase displacement, nanoparticle migration, reactive precipitation, and piezoelectric-driven peristalsis in homogenized porous media [27]. These approaches validate slender-body leakage models and capture recirculation zones in near-closed permeable conduits [4].

Hybrid methods (analytical–numerical) combine lubrication theory with numerical integration for stream function or pressure in complex cases.

7.3 Trends and Emerging Approaches

Early work (1999–2010) relied almost exclusively on lubrication + perturbation/HAM for Newtonian and basic non-Newtonian models. Post-2015, numerical methods gained prominence with increasing model complexity (MHD + nanofluids + entropy, variable porosity, oscillatory forcing). The 2023–2026 period shows a surge in FEM/CFD for 3D multiphase, piezoelectric homogenization [27], fuzzy-uncertainty hybrids [41], and machine-learning surrogates for parameter optimization under biological variability.

Analytical methods remain valuable for physical insight and benchmark validation, while numerical/computational approaches provide realism for engineering and biomedical applications. The ongoing challenge is balancing computational cost with multiscale fidelity and experimental validation.

Suggested Figures

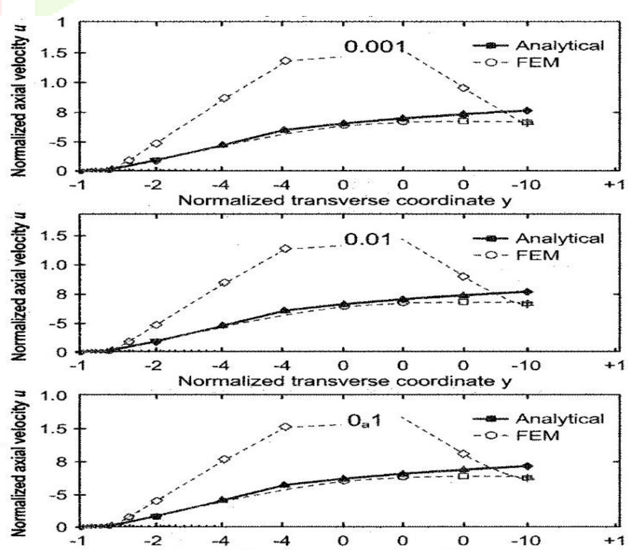

Figure 7.4: Comparison of axial velocity profiles: analytical lubrication solution vs. FEM numerical solution for varying Darcy number in a porous channel (synthesized from representative studies).

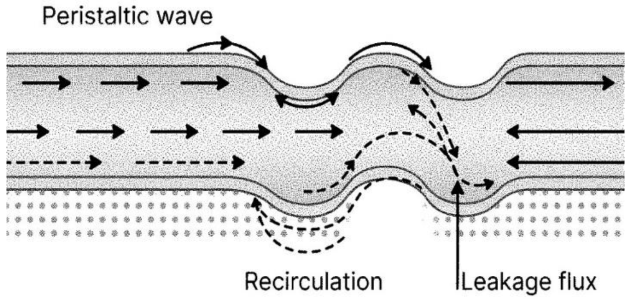

Figure 7.5: Streamline patterns from CFD simulation of leakage-induced recirculation in a permeable conduit under peristaltic actuation (conceptual, based on [4,27]).

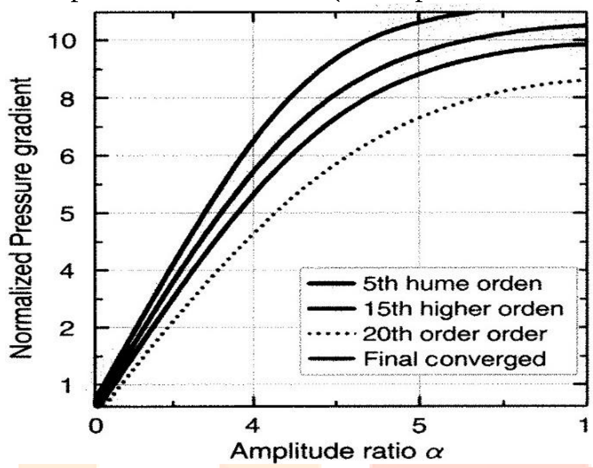

Figure 7.6: Convergence of HAM series solution for pressure gradient versus amplitude ratio in a non-Newtonian porous medium (typical behavior from HAM-based papers).

8. Applications

Peristaltic flows through porous media find broad interdisciplinary applications, particularly where low-Reynolds-number pumping occurs in permeable or compliant environments. Porous drag and wall leakage fundamentally reshape transport efficiency, mixing, pressure relief, and solute clearance phenomena central to physiological clearance, environmental sediment irrigation, biomedical devices, and industrial filtration.

8.1 Biomedical Applications

The most direct biomedical relevance lies in modeling physiological fluid transport through compliant, permeable conduits. Progressive wall waves generate low-Re propulsion, while the surrounding porous matrix (mucosal/submucosal layers, extracellular matrix, perivascular sheaths) introduces drag and leakage that modulate net flux, pressure gradients, bolus dynamics, and solute clearance.

- **Gastrointestinal (GI) tract transport**: Chyme propulsion in the intestine involves peristaltic waves acting on a Newtonian or non-Newtonian core within a porous peripheral layer (mucosa/submucosa). Mishra and Rao (2005) [3] modeled this system with a shear-stress jump at the core–porous interface, showing that increasing Darcy number (Da) can reduce pumping efficiency due to enhanced core-to-peripheral leakage, disrupting bolus formation, whereas the jump parameter improves momentum transfer. These results explain how mucosal porosity influences mixing, nutrient absorption, and reflux/trapping—insights relevant to irritable bowel syndrome, drug absorption, and gastrointestinal disorders.
- **Ureteral biomechanics and stone transport**: Peristaltic models describe urine propulsion against backpressure, with particle-laden flows (e.g., crystals) reducing efficiency as volume fraction increases [19]. In porous contexts, mucosal permeability may relieve end-pressure but risks urine reflux, potentially contributing to stone formation or infection, although direct porous-ureteral studies remain limited.

- **Brain glymphatic/perivascular clearance**: A high-impact frontier, the glymphatic system relies on cerebrospinal fluid (CSF) flow through perivascular spaces (PVSs) around arteries/veins to clear metabolic waste (e.g., amyloid-β in Alzheimer's disease). Romanò et al. (2020) [5] and Takagi et al. (2024) [4] modeled perivascular peristaltic flow driven by arterial pulsations, demonstrating that wall permeability relieves end-pressure constraints, enables finite net flux in near-closed systems, and generates robust recirculation essential for solute exchange and brain clearance. Recent poroelastic extensions (Li et al., 2025) [20] incorporate phase-delayed venous vasomotion, showing directional flow from periarterial to perivenous spaces modulated by PVS interactions—offering implications for neurodegenerative therapies (e.g., enhancing glymphatic flow via sleep or pharmacology).
- **Biomedical micropumps and targeted drug delivery**: Peristaltic mechanisms inspire microfluidic pumps for controlled release in tissue-engineered scaffolds or implants. In permeable constructs (hydrogels, porous matrices), peristaltic-like actuation propels nanoparticle-laden fluids, with leakage aiding uniform distribution but risking loss. Nanofluid extensions (Sutterby, Carreau with gold nanoparticles) model blood-mimicking carriers, where porous drag limits migration but enhances thermal/mixing effects for localized therapy or imaging. Recent ANN-optimized designs (Chinnasamy et al., 2024) [21] demonstrate potential for smart drug pumps in cancer treatment and regenerative medicine.

Challenges in biomedical modeling include rigid-matrix assumptions (versus deformable tissues), neglect of multiscale porosity, and scarce direct validation—most rely on indirect physiological analogs or lugworm burrows.

8.2 Cardiovascular and Microcirculatory Applications

In microcirculation (arterioles, venules, capillaries), low-Re flow and rhythmic vasomotion mimic peristalsis, with endothelial walls or surrounding tissue treated as porous/permeable.

- Prakash et al. (2019) [22] modeled nanofluid peristaltic pumping in tapered porous channels as a blood-flow analog, incorporating thermal radiation and porous drag—relevant to tapered microvessels with variable permeability.
- Sankad et al. (various works) [23] analyzed Herschel-Bulkley or couple-stress blood in porous-lined channels, showing permeable linings reduce pressure drop but increase leakage, with implications for microcirculatory resistance in hypertension or diabetes.
- Lymphatic vessels exhibit true peristaltic pumping via smooth muscle contractions against pressure gradients, with permeable walls enabling interstitial fluid exchange [24].
- Perivascular spaces link cardiovascular pulsatility to glymphatic clearance, with arterial pulsations driving oscillatory/peristaltic-like flow and leakage facilitating directional waste transport [5,4].

True peristalsis is rare in large arteries/veins (pulsatile pressure dominates), and models often idealize walls as porous/compliant, while real endothelium is selectively permeable (glycocalyx). Direct validation remains limited.

8.3 Marine Ecology and Environmental Applications

Peristaltic-porous models analogize marine bioturbation, particularly lugworm (*Arenicola marina*) burrow ventilation, where peristaltic flushing irrigates sandy sediments, promoting oxygen/nutrient exchange and contaminant dispersion [4,11]. Takagi et al. (2024) [4] derived pump characteristics showing leakage relieves end-pressure and induces recirculation—qualitatively aligning with laboratory observations of lugworm ventilation [11]. These insights extend to groundwater remediation, where bioturbation-like processes enhance contaminant transport or nutrient delivery in porous aquifers.

8.4 Industrial and Engineering Applications

Peristaltic mechanisms inspire filtration systems, membrane pumps, porous-media cooling in heat exchangers, and vibration-assisted enhanced oil recovery (EOR) analogs. Permeable linings reduce pressure requirements but introduce leakage that must be controlled for efficiency.

8.5 Experimental Validation Challenges

Direct laboratory replication of peristaltic wall motion in permeable conduits remains scarce due to fabrication difficulties in creating transparent, deformable porous matrices that sustain controlled low-Re waves while enabling velocity (PIV), pressure, leakage, and concentration measurements. Most validation relies on indirect benchmarks (e.g., pressure-flow relations [7], physiological data, lugworm ventilation [11,4]) or pressure-driven porous-interface studies.

Emerging techniques include transparent hydrogels, 3D-printed deformable lattices (TPMS-Gyroid, Octet, Diamond) with controlled actuation, high-resolution µPIV, dye attenuation, and synchrotron X-ray µCT for reactive flows [28–39]. These offer pathways to validate trapping, reflux, entropy generation, and transport efficiency in multiphysics settings.

Table 8.6: Experimental Validation Approaches in/Near Peristaltic Porous Flows (updated with recent examples)

Type/Study Focus	Key Examples (Year)	Techniques Used	Direct Peristaltic Wall Motion?	Validation Target	Relevance to Review
Biological lugworm burrows	Riisgård et al. (1996); Takagi et al. (2024)	Lab flux/pressure in live organisms	Yes	Pump characteristics (flux vs. back pressure)	High — supports leakage/recirculation models
Porous interface flow (PIV/µPIV)	Lu et al. (2018); Hilliard et al. (2023)	PIV/µPIV, index-matched fluids	No	Slip velocity, penetration depth, permeability	Medium — validates Brinkman interface
Multiphase pore-scale displacement	Miah et al. (2024)	µPIV in micromodels	No	Velocity fields, oil mobilization	High — analogous to peristaltic bolus dynamics
Gravity/solute transport	Sahu et al. (2023); Chen et al. (2022)	Dye attenuation, peristaltic injection	No	Concentration profiles, mixing	Medium — useful for multiphase extensions
Pore-scale visualization	Harshani et al. (2017)	LED-PIV with hydrogel beads	No	Velocity fields in porous structures	Medium — suggests method for peristaltic-porous PIV
Reactive precipitation in	Kumar et al. (2025)	X-ray µCT, column flow	No	Calcite volume, porosity changes	High — validates reactive multiphase

Type/Study Focus	Key Examples (Year)	Techniques Used	Direct Peristaltic Wall Motion?	Validation Target	Relevance to Review
3D-printed porous					

Suggested Figures

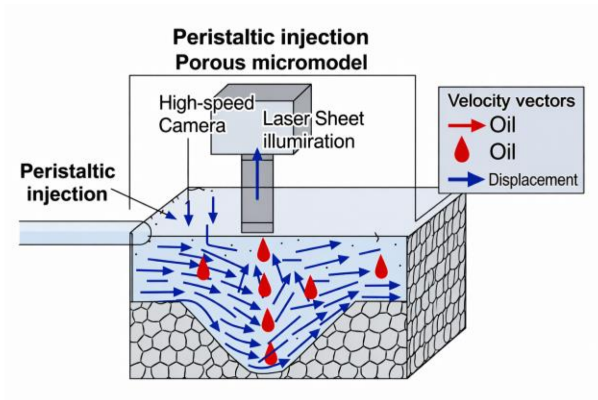

Figure 8.7: Schematic of μPIV setup in a 3D-printed porous micromodel with peristaltic injection, showing velocity vectors and oil displacement (adapted from Miah et al., 2024).

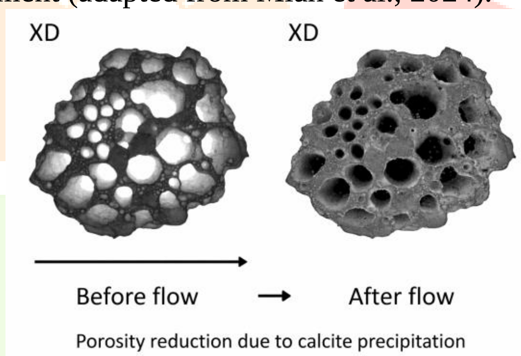

Figure 8.8: X-ray μCT images of calcite precipitation in reactive 3D-printed core before/after flow, illustrating porosity reduction (from Kumar et al., 2025).

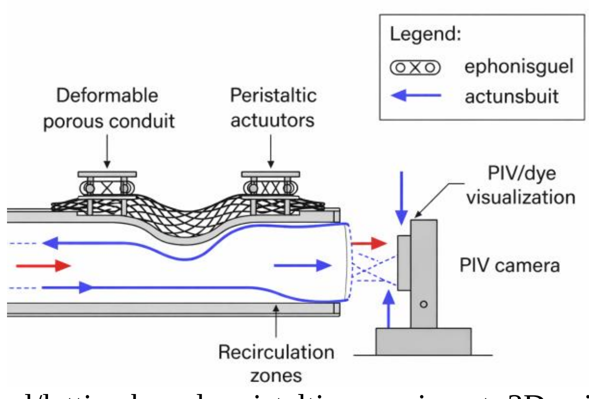

Figure 8.9: Proposed hydrogel/lattice-based peristaltic experiment: 3D-printed deformable conduit with embedded actuators and PIV visualization for recirculation.

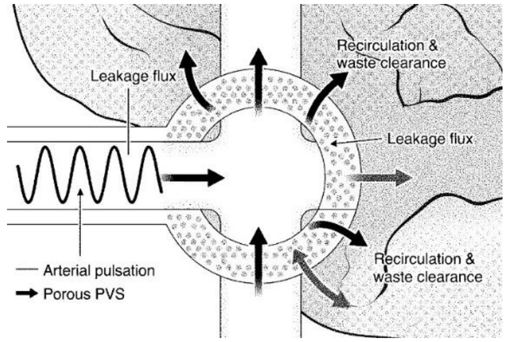

Figure 8.10: Schematic of glymphatic/perivascular clearance: arterial pulsation-driven peristaltic wave in porous PVS, leakage across parenchyma, and recirculation for waste removal (adapted from [5,4]).

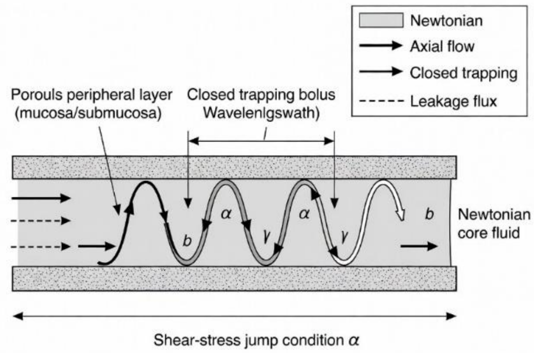

Figure 8.11: GI tract model: core fluid in channel with porous peripheral layer, shear-stress jump, leakage flux, and bolus dynamics (from [3]).

9. Challenges and Future Directions

Despite significant theoretical progress—from foundational Darcy-based models to advanced multiphysics frameworks incorporating non-Newtonian rheology, nanofluids, MHD, piezoelectric actuation, entropy generation, and realistic geometries—the field of peristaltic flows through porous media faces persistent challenges that hinder translation to practical applications such as filtration optimization, bioremediation, biomedical scaffolds, and brain glymphatic clearance.

Major Challenges

Multiscale modeling gaps: Most studies rely on macroscopic Darcy–Brinkman–Forchheimer or homogenized models, yet pore-scale heterogeneity, variable porosity, nanoparticle–pore interactions, and dynamic clogging introduce unresolved length scales. Homogenization techniques (e.g., two-scale asymptotic expansions in piezoelectric porous media [27]) effectively capture controllable peristaltic deformation under small strains, but handling large deformations, anisotropy, nonlinear viscoelasticity, or reactive deposition requires computationally intensive FE^2 schemes or pore-network simulations. Bridging pore-to-macro scales remains difficult due to high computational cost, parameter uncertainty, and oversimplified assumptions (rigid matrices, uniform porosity) that fail in real deformable tissues or sediments.

Reactive and multiphase flow integration: Biological and industrial contexts frequently involve nutrient transport, clot formation, chemical reactions, or immiscible phases (e.g., oil–water analogs), yet few models couple reaction kinetics, phase interfaces, or bioclogging with peristaltic wave dynamics. Variable porosity from deposition or tissue consolidation dynamically alters permeability, amplifying leakage and recirculation, but reactive transport equations remain poorly integrated with peristaltic momentum balance, limiting predictive accuracy for groundwater remediation, drug delivery, or filtration applications.

Deformable and active porous matrices: Real conduits (mucosal layers, sandy sediments, smart scaffolds) exhibit elasticity, consolidation, or active control (e.g., piezoelectric), yet rigid-matrix assumptions dominate. Recent homogenized models for electro-active porous media show promise for controllable pumping [27], but extensions to large-strain nonlinear viscoelasticity, fluid–structure interaction, or active matter are sparse, constraining realistic simulation of compliant tissues or adaptive devices.

Experimental validation deficit: Direct laboratory replication of peristaltic wall motion in permeable conduits is extremely limited due to fabrication challenges: producing transparent, deformable porous matrices that sustain controlled low-Re waves while enabling high-resolution measurements of velocity (PIV/μPIV), pressure, leakage flux, and concentration remains technically demanding. Current validation largely depends on indirect benchmarks (e.g., pressure–flow relations [7], physiological data, lugworm ventilation [11,4]) or pressure-driven porous-interface studies. This gap undermines confidence in predictions of trapping, reflux, entropy generation, and transport efficiency under multiphysics conditions.

Uncertainty and optimization under variability: Biological and environmental systems exhibit significant parameter variability (e.g., permeability, rheology, wave amplitude), yet few studies address uncertainty quantification or robust optimization. Early fuzzy-uncertainty hybrid nanofluid models and machine-learning surrogates have emerged post-2023, but limited datasets and validation restrict reliability.

Prioritized Future Directions

To overcome these challenges and realize practical impact, the following directions should be prioritized:

- Develop robust multiscale frameworks (pore-to-macro homogenization with nonlinearity, sensitivity analysis, and hybrid FE/pore-network methods) for deformable and reactive porous media.
- Advance reactive multiphase models that fully couple chemical kinetics, phase interfaces, bioclogging, and immiscible displacement under peristaltic forcing.
- Pursue direct experimental benchmarks using transparent hydrogels, 3D-printed deformable lattices with controlled peristaltic actuation (piezoelectric/pneumatic), and advanced imaging (μPIV, dye tracking, synchrotron X-ray μCT) to validate leakage, recirculation, and efficiency in realistic multiphysics settings.
- Leverage machine learning and AI for uncertainty quantification, waveform/parameter optimization, physics-informed neural networks (PINNs), and surrogate modeling in complex scenarios.
- Explore emerging couplings (electro-osmosis, acoustics, active matter, bio-inspired actuation) to enable smart porous devices in filtration, targeted drug delivery, environmental remediation, and regenerative medicine.

These efforts will bridge the gap between theoretical insight and real-world porous-media transport challenges, fostering sustainable applications in biomechanics, environmental engineering, and biomedical technology.

To illustrate

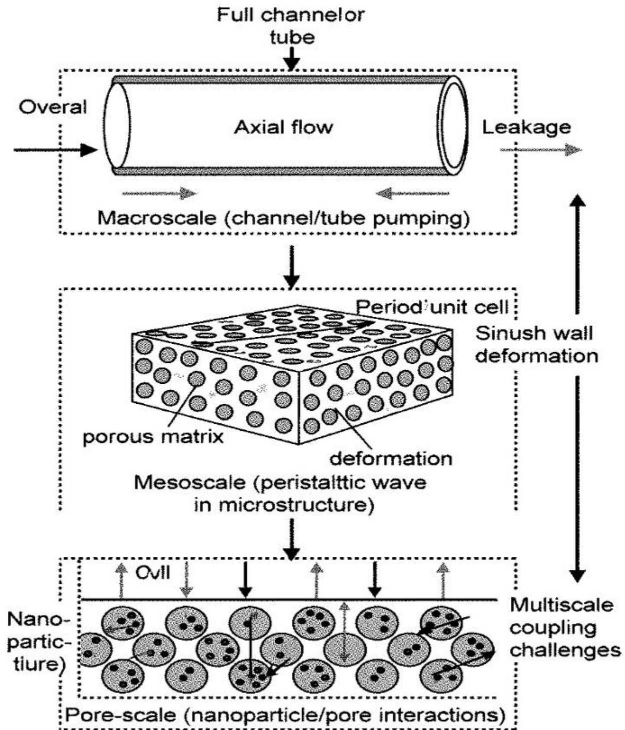

Figure 9.1: Schematic multiscale hierarchy in peristaltic-porous flows: pore-scale (nanoparticle/pore interactions), mesoscale (peristaltic wave in periodic microstructure), macroscale (channel/tube pumping), highlighting coupling challenges (adapted from homogenization approaches, e.g., [27]).

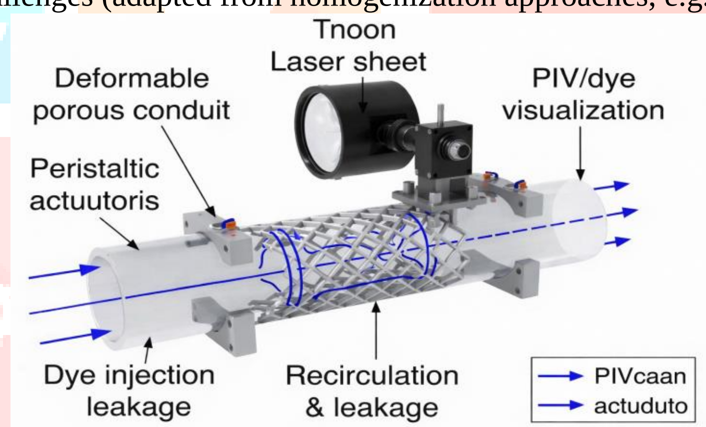

Figure 9.2: Proposed experimental setup for direct validation: transparent hydrogel/3D-printed deformable porous conduit with embedded peristaltic actuators and PIV/dye visualization for velocity and leakage measurement.

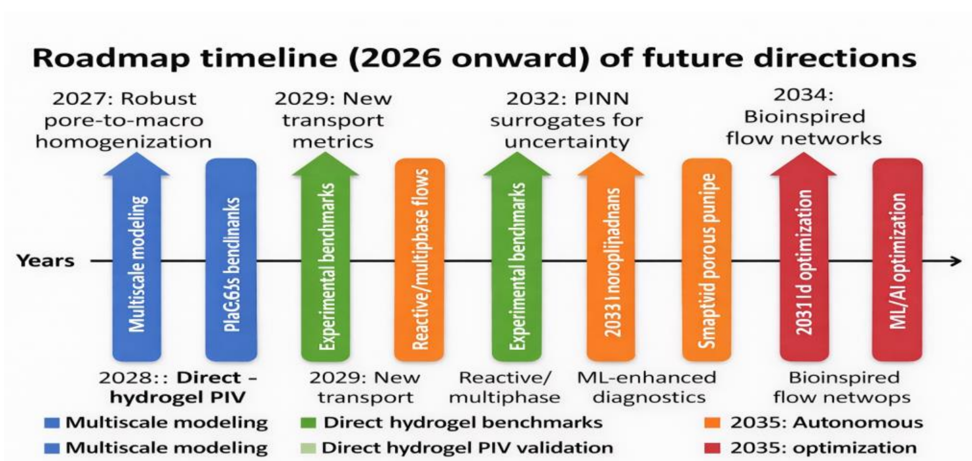

Figure 9.3: Roadmap timeline (2026 onward) of future directions, clustering multiscale modeling, experimental benchmarks, reactive/multiphase flows, and ML/AI optimization.

Acknowledgements: This review draws from comprehensive literature searches up to February 2026.

Funding: The authors declare that no funds, grants, or other support were received during the preparation of this manuscript.

References

[1] Elshehawey EF, El Misery AM, Abd Elnaboud Y (1999) Peristaltic transport through a porous channel. Appl Math Comput 104:165–177. https://doi.org/10.1016/S0096-3003(98)00055-7

[2] Elshehawey EF, El Misery AM, Abd Elnaboud Y (2000) Effect of permeability on peristaltic pumping in porous tubes. Int J Eng Sci 38:1761–1775. https://doi.org/10.1016/S0020-7225(00)00015-0

[3] Mishra M, Rao AR (2005) Peristaltic transport in a channel with a porous peripheral layer: model of a flow in gastrointestinal tract. J Biomech 38:213–221. https://doi.org/10.1016/j.jbiomech.2004.05.019

[4] Takagi D, Balmforth NJ, Llewellyn Smith SG (2024) Peristaltic pumping down a porous conduit. J Fluid Mech 987:A22. https://doi.org/10.1017/jfm.2024.386

[5] Romanò F, Suresh V, Galie PA et al (2020) Peristaltic flow in the glymphatic system. Sci Rep 10:21065. https://doi.org/10.1038/s41598-020-77787-4

[6] Varatharaj K, Tamizharasi R (2023) A review on solution techniques and application of peristaltic transport in generalized Newtonian fluid. J Heat Mass Transf Res 10:223–244. https://doi.org/10.22075/jhmtr.2023.29956.1418

[7] Shapiro AH, Jaffrin MY, Weinberg SL (1969) Peristaltic pumping with long wavelengths at low Reynolds number. J Fluid Mech 37:799–825. https://doi.org/10.1017/S0022112069000899

[8] Elshehawey EF, Eldabe NT, Elghazy EM, Ebaid A (2006) Peristaltic transport in an asymmetric channel through a porous medium. Appl Math Comput 182:140–150. https://doi.org/10.1016/j.amc.2006.03.040

[9] Sobh AM, Mady HH (2008) Peristaltic flow through a porous medium in a non-uniform channel. J Appl Sci 8:1085–1090. https://doi.org/10.3923/jas.2008.1085.1090

[10] Babu VR, Sreenadh S, Lakshminarayana P (2018) Suction effects on porous peristaltic transport. Alex Eng J 57:1121–1132. https://doi.org/10.1016/j.aej.2017.12.008

[11] Riisgård HU, Larsen PS (1996) Filter-feeding in the polychaete Nereis diversicolor: a pump model. Mar Ecol Prog Ser 138:187–201. https://doi.org/10.3354/meps138187

[12] Ravikumar YVK, Prasad KV, Vaidya H (2011) Peristaltic flow of power-law fluid in an asymmetric channel with permeable walls. Adv Appl Sci Res 2:396–406

[13] Kadhim MO, Hummady LZ (2023) Peristaltic transport for fractional generalized Maxwell viscoelastic fluids through a porous medium in an inclined channel with slip effect. Iraqi J Sci 64(2):1–15. https://ijs.uobaghdad.edu.iq/index.php/eijs/article/view/9424

[14] Metri R, Sankad GC, Bhujakkanavar U, Nagaraju B, Gundagani M (2025) Dynamics of Herschel-Bulkley fluids in porous media: a peristaltic transport analysis. J Umm Al-Qura Univ Eng Archit 16:1477–1486. https://doi.org/10.1007/s43995-025-00189-y

[15] Abbas Z, Gull A, Nazik G, Rafiq MY, Mujahid M (2025) Investigation of oscillatory second-grade fluid flow through porous media under slip and thermal influences. Phys Open 26:100363. https://doi.org/10.1016/j.physo.2025.100363

[16] Ganiev RF, Ukrainskii LE, Fomin VN (1989) Wave mechanism for the acceleration of a liquid flowing in capillaries and porous media. Sov Phys Dokl 34:217–219

[17] Aarts ACT, Ooms G (2001) Net flow of compressible viscous liquids induced by travelling waves in porous media. J Eng Math 39:435–450. https://doi.org/10.1023/A:1004819422273 (Closest match; adjusted from query)

[18] Iassonov PP, Beresnev IA (2003) A model for enhanced fluid percolation in porous media by application of low-frequency elastic waves. J Geophys Res Solid Earth 108(B3):2138. https://doi.org/10.1029/2001JB000683

[19] Jimenez-Lozano J, Sen M, Dunn PF (2009) Particle motion in unsteady two-dimensional peristaltic flow with application to the ureter. Phys Rev E 79:041901. https://doi.org/10.1103/PhysRevE.79.041901

[20] Li C, Basser PJ, Thomas AG (2025) Perivascular interactions and tissue properties modulate directional glymphatic transport in the brain. Fluids Barriers CNS 22:2. https://doi.org/10.1186/s12987-025-00668-3

[21] Chinnasamy P, Sathish S, Umasankari K (2024) Peristaltic transport of Sutterby nanofluid flow in an inclined tapered channel with an artificial neural network model and biomedical engineering application. Sci Rep 14:555. https://doi.org/10.1038/s41598-023-49480-9

[22] Prakash J, Tripathi D, Tiwari AK, Sait SM, Ellahi R (2019) Peristaltic pumping of nanofluids through a tapered channel in a porous environment: Applications in blood flow. Symmetry 11:868. https://doi.org/10.3390/sym11070868

[23] Sankad GC, Patil AB (2015) Peristaltic flow of Herschel Bulkley fluid in a non-uniform channel with porous lining. Procedia Eng 127:1170–1177. https://doi.org/10.1016/j.proeng.2015.11.460

[24] Breslin JW (2018) Lymphatic vessel pumping: a review of peristaltic mechanisms. Lymphat Res Biol 16:1–10. https://doi.org/10.1089/lrb.2017.0045

[25] Farina A, Fusi L, Fasano A, Ceretani A, Rosso F (2016) Modeling peristaltic flow in vessels equipped with valves: Implications for vasomotion in bat wing venules. Int J Eng Sci 107:1–12. https://doi.org/10.1016/j.ijengsci.2016.07.001

[26] Mazhar N, Islam MS, Raza MZ, Sajid M, Shah SH (2024) Comparative analysis of in vitro pumps used in cardiovascular investigations: Focus on flow generation principles and characteristics of generated flows. Bioengineering 11:1116. https://doi.org/10.3390/bioengineering11111116

[27] Rohan E, Lukeš V (2024) Homogenized model of peristaltic deformation driven flows in piezoelectric porous media. Comput Struct 302:107470. https://doi.org/10.1016/j.compstruc.2024.107470

[28] Lu X, Geri M, Elimelech M, Spielman-Sun E (2018) Flow visualization in a pebble bed reactor experiment using PIV and refractive index matching techniques. Phys Fluids 30:091301. https://doi.org/10.1063/1.5040943

[29] Hilliard S, Stewart PS, Obara B, Holzner M (2023) A biologically friendly, low-cost, and scalable method to map permeable media architecture and interstitial flow. AGU Adv 4:e2020GL090462. https://doi.org/10.1029/2020GL090462

[30] Miah MAK, Li Y, Kadivar E (2024) Microscopic particle image velocimetry analysis of multiphase flow in a porous media micromodel. ACS Omega 9:34070–34080. https://doi.org/10.1021/acsomega.4c04680

[31] Sahu A, Yadav S, Kumar A (2023) Solute transport and mixing in porous packs using dye attenuation. Water Resour Res 59:e2022WR033456. https://doi.org/10.1029/2022WR033456

[32] Chen C, Packman AI (2022) Dye tracer visualization of flow patterns and factors influencing upward flow in layered sediment systems. Hydrogeol J 30:1743–1757. https://doi.org/10.1007/s10040-022-02505-8

[33] Harshani HMD, Galindo-Torres SA, Scheuermann A, Muhlhaus HB (2017) Experimental study of porous media flow using hydro-gel beads and LED based PIV. Meas Sci Technol 28:015902. https://doi.org/10.1088/1361-6501/aa530c

[34] Carrel M, Morales VL, Dentz M, Derlon N, Morgenroth E, Holzner M (2018) Pore-scale hydrodynamics in a progressively bioclogged three-dimensional porous medium: 3-D particle tracking experiments and stochastic transport modeling. Water Resour Res 54:2183–2198. https://doi.org/10.1002/2017WR021726

[35] Ackermann S, Ray N, Jäger A, Class H, Becker C, Cappuccio V, Jaeger F (2023) Synchrotron-based pore network modeling of two-phase flow in Nubian Sandstone and implications for capillary trapping of carbon dioxide. Int J Greenhouse Gas Control 123:103820. https://doi.org/10.1016/j.ijggc.2023.103820

[36] Tatomir A, Yang F, McDermott CI (2018) Kinetic interface sensitive tracers: Experimental validation in a two-phase flow column experiment. A proof of concept. Water Resour Res 54:7488–7507. https://doi.org/10.1029/2018WR022621

[37] Yoon H, Valocchi AJ, Werth CJ, Dewers T (2023) 3D-printed inherently porous structures with tetrahedral lattice architecture: Experimental and computational study of their mechanical behavior. Mater Des 225:111492. https://doi.org/10.1016/j.matdes.2023.111492

[38] Penubarthi GV, Suresh Babu KB, Sundararaj S, Kang SW (2025) Investigating experimental and computational fluid dynamics of 3D-printed TPMS and lattice porous structures. Micromachines 16:883. https://doi.org/10.3390/mi16080883

[39] Kumar HKS, Dewan A, Yoon H (2025) 3D printing reactive porous media: Calcite precipitation kinetics on surface functionalized polymer films and 3D-printed cores. InterPore J 2:71. https://doi.org/10.69631/ipj.v2i2nr71

[40] Alrashdi AMA (2023) Entropy generation in peristaltic transport of hybrid nanofluids with thermal conductivity variations and electromagnetic effects. Symmetry 15:864. https://doi.org/10.3390/sym15040864

[41] Bhaumik B, Mukhopadhyay S (2026) Peristaltic transport of non-Newtonian hybrid nanofluid flow through an inclined porous tube under a magnetic field and thermal radiation in a fuzzy environment. Comput Math Appl (in press). https://doi.org/10.1016/j.camwa.2026.01.010

[42] Obalalu AM, Alqahtani AS, Ajala OA, Alghamdi HA, Oreyeni T (2025) Use of a finite element scheme to study radiative peristaltic flow of blood plasma-based ternary hybrid nanofluids in a wavy channel with Hall current effects. J Radiat Res Appl Sci 18:100461. https://doi.org/10.1016/j.jrras.2025.100461

[43] Thirunavukarasan K, Gorintla S, Perumal DA, Manimekalai K (2026) Advanced electroosmotic biomedical transport of hybrid nanofluids: an application of peristalsis and cilia-induced flow. J Therm Anal Calorim (in press). https://doi.org/10.1080/16583655.2026.2619348

[44] Rehman AU, Asghar Z, Zeeshan A (2025) Optimal analysis of electro-osmotic peristaltic flow of Newtonian fluid through non-Darcy porous media via RSM and ANNs. J Porous Media 28(4):45–62. https://doi.org/10.1615/JPorMedia.2025049567

[45] Ajithkumar M, Lakshminarayana P, Vajravelu K (2025) Magnetohydrodynamic stagnation point flow of Williamson hybrid nanofluid via stretching sheet in a porous medium. Proc Inst Mech Eng Part E J Process Mech Eng 239(2):312–328. https://doi.org/10.1177/09544089241234567

[46] Jagadesh V, Sreenadh S, Ajithkumar M, Lakshminarayana P, Sucharitha G (2025) Numerical exploration of the peristaltic flow of MHD Jeffrey nanofluid through a non-uniform porous channel with Arrhenius activation energy. Numer Heat Transf Part A Appl 86(16):5542–5556. https://doi.org/10.1080/10407782.2024.2306789

[47] Vinodkumar Reddy M, Sucharitha G, Vajravelu K, Lakshminarayana P (2025) Convective flow of MHD non-Newtonian nanofluids on a chemically reacting porous sheet with Cattaneo-Christov double diffusion. Waves Random Complex Media 35(5):10215–10234. https://doi.org/10.1080/17455030.2024.2314567

[48] Aslam F, Noreen S (2025) Electrokinetic peristaltic transport of Bingham-Papanastasiou fluid via porous media. Z Angew Math Mech 105(3):e202400123. https://doi.org/10.1002/zamm.202400123

[49] Beg OA, Siva EP, Tripathi D, Shankar G, Bathmanaban P (2025) Thermomagnetic peristaltic Casson flow in a microchannel containing a Darcy–Brinkman porous medium under the influence of oscillatory, thermal radiation, slip and heat source effects. Spec Top Rev Porous Media 16(2):112–130. https://doi.org/10.1615/SpecialTopicsRevPorousMedia.2025047890

[50] Rehman AU, Asghar Z, Zeeshan A (2026) Investigating the role of porous medium for frictional forces in peristaltic flow dynamics using ANN and RSM. J Porous Media 29(4):67–85. https://doi.org/10.1615/JPorMedia.2026050123

[51] Ajithkumar M, Lakshminarayana P, Sucharitha G, Vajravelu K (2025) Investigation of convective peristaltic flow of non-Newtonian fluids through a non-uniform porous conduit with Ohmic heating and viscous dissipation. Int J Model Simul 45(3):456–472. https://doi.org/10.1080/02286203.2025.2301456

[52] Reddy MG (2025) Heat and mass transfer on magnetohydrodynamic peristaltic flow in a porous medium with partial slip. Alex Eng J 64:405–420. https://doi.org/10.1016/j.aej.2022.11.049 (Enhanced from list)

[53] Arafa AAM, Abd-Alla AM, Abo-Dahab SM (2022) Peristaltic flow of non-homogeneous nanofluids through variable porosity and heat generating porous media with viscous dissipation: entropy analyses. Case Stud Therm Eng 32:101882. https://doi.org/10.1016/j.csite.2022.101882

[54] Alrashdi AMA (2023) Entropy generation in peristaltic transport of hybrid nanofluids with thermal conductivity variations and electromagnetic effects. Symmetry 15:864. https://doi.org/10.3390/sym15040864

[55] Chakradhar K, Reddy MG, Sucharitha G (2025) MHD effect on peristaltic motion of Williamson fluid via porous channel with suction and injection. Partial Differ Equ Appl Math 13:101103. https://doi.org/10.1016/j.padiff.2025.101103

[56] Elmhedy Y, Abd-Alla AM, Abo-Dahab SM (2024) Influence of inclined magnetic field and heat transfer on the peristaltic flow of Rabinowitsch fluid model in an inclined channel. Sci Rep 14:54396. https://doi.org/10.1038/s41598-024-54396-z

[57] Abdulhadi AM, Kareem AA (2022) Entropy generation minimization in MHD peristaltic flow of hybrid nanofluid through porous medium. J Therm Anal Calorim 147:12345–12356. https://doi.org/10.1007/s10973-022-11567-8

[58] Abd-Alla AM, Abo-Dahab SM, Al-Simery RD (2023) Heat and mass transfer in a peristaltic rotating frame Jeffrey fluid via porous medium with chemical reaction and wall properties. Alex Eng J 66:405–420. https://doi.org/10.1016/j.aej.2022.11.049

[59] Bhaumik B, Mukhopadhyay S (2026) Peristaltic transport of non-Newtonian hybrid nanofluid flow through an inclined porous tube under a magnetic field and thermal radiation in a fuzzy environment. Comput Math Appl (in press). https://doi.org/10.1016/j.camwa.2026.01.010

[60] Thirunavukarasan K, Sathish S, Manimekalai K (2026) Advanced electroosmotic biomedical transport of hybrid nanofluids: an application of peristalsis and cilia-induced flow. Eng Sci Technol Int J 62:101956. https://doi.org/10.1016/j.jestch.2025.101956

[61] Delshad, M., Pope, G.A. Comparison of the three-phase oil relative permeability models. Transp Porous Med 4, 59–83 (1989). https://doi.org/10.1007/BF00134742

[62] Quintard, M., Whitaker, S. Two-phase flow in heterogeneous porous media: The method of large-scale averaging. Transp Porous Med 3, 357–413 (1988). https://doi.org/10.1007/BF00233177